

# Tunable photonic Bloch oscillations in electrically modulated photonic crystals

Gang Wang,<sup>1,2</sup> Ji Ping Huang,<sup>1,2,\*</sup> and Kin Wah Yu<sup>1,\*\*</sup>

<sup>1</sup>*Department of Physics, Chinese University of Hong Kong, Shatin, New Territories, Hong Kong*

<sup>2</sup>*Surface Physics Laboratory and Department of Physics, Fudan University, Shanghai 200433, China*

\**Corresponding author: jphuang@fudan.edu.cn*

\*\**Corresponding author: kwyu@phy.cuhk.edu.hk*

We exploit theoretically the occurrence and tunability of photonic Bloch oscillations (PBOs) in one-dimensional photonic crystals (PCs) containing nonlinear composites. Because of the enhanced third-order nonlinearity (Kerr type nonlinearity) of composites, photons undergo oscillations inside tilted photonic bands, which are achieved by the application of graded external pump electric fields on such PCs, varying along the direction perpendicular to the surface of layers. The tunability of PBOs (including amplitude and period) is readily achieved by changing the field gradient. With an appropriate graded pump AC or DC electric field, terahertz PBOs can appear and cover a terahertz band in electromagnetic spectrum.

© 2008 Optical Society of America

*OCIS codes:* 230.4910, 350.4238, 350.5500.

Recently matter wave dynamics of Bloch oscillations has already motivated a good deal of attention. In 1928, Bloch made a striking prediction that in a crystal lattice, a homogeneous static electric field induces an oscillatory rather than uniform motion of the electrons [1], referred to as Bloch oscillations (BOs). Electronic BOs have been observed in semiconductor superlattices [2, 3]. Now this phenomenon has been extended to various classical wave systems, such as acoustic systems [4], elastic systems [5], and photonic systems [6]. The electronic BOs are quite easily tunable via externally applied electric fields or magnetic fields, or simultaneously by both [7]. However, for uncharged particles like photons, one has to resort to other approaches for controllability [8].

In this work, we propose a class of PCs to realize the occurrence and tunability of photonic Bloch oscillations (PBOs) by graded pump DC or AC electric fields  $\mathbf{E}_0$ . The idea relies on the fact that the effective dielectric permittivity (thus refractive index) of some materials depends on external electric fields because of the third-order nonlinearity (Kerr type nonlinearity). To exemplify this idea, we theoretically calculate the PBOs in such PCs under different graded pump electric fields. Compared with existing proposals [8], our proposal offers ultrafast response time and dynamical control. Also, we show that with an appropriate choice of parameters, this could lead to a generation of terahertz radiations.

Figure 1 shows a one-dimensional double-layer PC, which consists of alternative layers of composite materials [9] (or composites for short, e.g., Au/SiO<sub>2</sub>) and common dielectric (e.g., air). Through local field and resonant scattering effects in nanoparticles [10], the third-order nonlinearity of composites can be enhanced [10, 11].

Let us denote by  $\mathbf{D}_{0(1)}$  the response to pump (probe) field  $\mathbf{E}_{0(1)}$ . For weak nonlinearity under consideration, namely  $\chi^{(3)}|\mathbf{E}|^2 \ll \epsilon$ , the constitutive relation  $\mathbf{D} = \epsilon\mathbf{E} + \chi^{(3)}|\mathbf{E}|^2\mathbf{E}$  can be written as  $\mathbf{D} = \mathbf{D}_0 + \alpha\mathbf{D}_1$ , and  $\mathbf{E} = \mathbf{E}_0 + \alpha\mathbf{E}_1$ , where  $\alpha$  is a small parameter. Due to the weak nonlinearity limit, we apply the perturbation method [12] to express  $\mathbf{D}_0$  and  $\mathbf{D}_1$  in terms of  $\mathbf{E}_0$  and  $\mathbf{E}_1$ :  $\mathbf{D}_0 = (\epsilon + \chi^{(3)}|\mathbf{E}_0|^2)\mathbf{E}_0$ ,  $\mathbf{D}_1 = \epsilon\mathbf{E}_1 + \chi^{(3)}|\mathbf{E}_0|^2\mathbf{E}_1 + 2\chi^{(3)}\text{Re}[\mathbf{E}_0^*\mathbf{E}_1]\cos\theta\mathbf{E}_0$ . Since the pump field  $\mathbf{E}_0$  is much larger than the probe field  $\mathbf{E}_1$ , the response to the probe field  $\mathbf{D}_1$  is rather stable, and it is related to the angle  $\theta$  between the pump field ( $\mathbf{E}_0$ ) and the probe field ( $\mathbf{E}_1$ ). Without loss of generality, we assume  $\mathbf{E}_1 \parallel \mathbf{E}_0$  (see Fig. 1), which results in an effective dielectric constant for the probe field  $\tilde{\epsilon}_{eff} = \epsilon + 3\chi^{(3)}|\mathbf{E}_0|^2$ . So the dielectric constant  $\tilde{\epsilon}_p$  possessed by nonlinear nanoparticles can be expressed as

$$\tilde{\epsilon}_p = \epsilon_p + 3\chi_p^{(3)}|\mathbf{E}_p|^2 \approx \epsilon_p + 3\chi_p^{(3)}\langle|\mathbf{E}_p|^2\rangle, \quad (1)$$

where  $\epsilon_p$  denotes the linear (field-independent) dielectric permittivity,  $\chi_p^{(3)}$  the third-order nonlinear susceptibility of the nanoparticles,  $\mathbf{E}_p$  the local electric field inside the nanoparticle, and  $\langle\cdots\rangle$  the volume average of  $\cdots$ . Then, the effective nonlinear permittivity  $\tilde{\epsilon}_1$  of the layer of composites can be given by the Maxwell-Garnett approximation [10]

$$\frac{\tilde{\epsilon}_1 - \epsilon_h}{\tilde{\epsilon}_1 + 2\epsilon_h} = p \frac{\tilde{\epsilon}_p - \epsilon_h}{\tilde{\epsilon}_p + 2\epsilon_h}, \quad (2)$$

where  $\epsilon_h$  represents the dielectric permittivity of the host (which is assumed to be linear for simplicity), and  $p$  the volume fraction of nanoparticles. The volume-averaged local electric field  $\langle|\mathbf{E}_p|^2\rangle$  in the layer is given by [13, 14]

$$\langle|\mathbf{E}_p|^2\rangle = \frac{9|\epsilon_h|^2}{|(1-p)\epsilon_p + (2+p)\epsilon_h|^2}\mathbf{E}_0^2 \equiv \beta^2\mathbf{E}_0^2. \quad (3)$$

Thus the effective nonlinear response of the layer can be much enhanced.

For model calculations, we investigate the composite of Au/SiO<sub>2</sub> with volume fraction of Au nanoparticles  $p = 0.20$ . The dielectric permittivities of SiO<sub>2</sub> and air (dielectric layer) are taken to be  $\epsilon_h = 2.25\epsilon_0$  and  $\epsilon_{air} = \epsilon_0$ . The probe field can be much weaker in strength than the pump electric field, so that the dispersion (and loss) of the (much weaker) probe field can be neglected. Here we take  $\epsilon_p = -9.97\epsilon_0$  [13, 15], which is a real frequency-independent constant. This corresponds to a pump field produced by a laser source at 620 nm [13].

The existence of the enhanced Kerr nonlinearity enables us to modify photonic band structures of such PCs by applying pump electric fields [9]. Throughout this work, we use  $\chi_p^{(3)}E_0^2$  to indicate the strength of external pump electric field  $E_0$ . To obtain PBOs, we apply an external electric field with gradation profile  $\chi_p^{(3)}E_0^2 = gz + b$ , which can be adjusted to achieve different gradation profiles. In graded fields, the photonic band structures become depth-dependent, viz.,  $z$ -dependent (see Fig. 2), which can be evaluated via the transfer matrix method with  $g = 3.67 \times 10^{-4}$  and  $b = 1.33 \times 10^{-2}$ . The reason is easily understood. When the pump electric field acting on the layers of composites varies along the  $z$  direction, the effective dielectric permittivity of each composite layer grows monotonically, resulting in a refractive index gradient. By carefully examining the condition for the appearance of PBOs, we are convinced that PBOs cannot happen in the lowest band. Thus we will study PBOs in the second (or higher) band. Besides the tilted band structures in Fig. 2, the other prerequisite for the appearance of PBOs is that  $\omega(z_{max}, k = 0) = \omega(z_{min}, k = \pi/a)$ , where  $\omega$  represents the angular frequency of source waves,  $z_{max(min)}$  means the maximum (minimum) position for PBOs, and  $k$  is the Bloch wave vector. In other words, PBOs just appear within the cross section that is composed by the two horizontal dotted lines as displayed in Fig. 2. So when the incidence with  $\omega_0 = 1.76 c/a$  illuminates the structure (see the arrow in Fig 2), the oscillations occur in the spatial range  $250a < z < 500a$ , in good agreement with the numerical results shown in Fig. 3 (a).

The above analysis shows that PBOs can appear inside the second band if a graded external electric field is applied on such 1D PCs. When electromagnetic waves are incident on the PCs, multiple reflections on the gaps lead to spatial BOs. The actual calculation is to solve for the propagation of a Gaussian wavepacket initially peaked around  $z = z_{max}$  and  $k = 0$  at  $t = 0$ . The subsequent motion of the wavepacket is governed by the Hamiltonian equations of motion of  $\omega(z, k)$ . At  $t = T_B/2$  ( $T_B$ : time period of PBOs),  $z$  becomes  $z_{min}$  while  $k$  reaches  $\pi/a$  and PBO occurs. The Hamiltonian equations of motion of  $\omega(z, k)$  have been integrated with appropriate initial conditions to yield the time series of displacement  $z(t)$  and momentum  $k(t)$  (not shown herein). As expected, such oscillations are clearly seen from the mean position  $\langle z(t) \rangle$  in Fig. 3 (a) and (b). For the use and justification of the Hamiltonian formalism for optics, please see Ref. [16] and references therein. Based on the semiclassical solutions, we access the width  $\Delta z(t)$  of a wave packet and show that it remains

bound in time. For a packet with Gaussian distribution with widths  $\sigma_z = 5$  and  $\sigma_k = 0.2$ , we show the time dependent mean width  $\Delta z(t)$  Fig. 3 (c) and (d). We can find that the width is about 5% of the length of the superlattice ( $600a$ ) and increases only slightly after several periods, which is acceptable. This originates from the non-constant inclination of the band diagram. Thus we can be convinced that Bloch oscillation indeed occurs. In fact, we can design linearly tilted bands to avoid the increase of the width.

The enhancement of the third-order nonlinearity of the composites enables us to tune PBOs by using tunable inclined band structures. Figure 3 shows the spatial range of PBOs for a fixed incident frequency  $\omega_0 = 1.76 c/a$  under different gradation profiles. We find that the variation of gradient plays an important role in the occurrence of PBOs, including their amplitude and oscillation frequency. A key parameter for PBOs is oscillation period  $T_B$ . Figure 3 also shows that  $T_B$  depends on the tuning parameters in the gradation profiles. Apparently,  $T_B$  decreases while increasing the field gradient because of steeper tilting bands. Therefore, there is a critical gradient  $g = 2.73 \times 10^{-4}$ , below which  $T_B$  becomes infinite (or, alternatively, no oscillations come to appear).

Considering the large nonlinear susceptibility (typical value  $8 \times 10^{-8}$  esu) of Au nanoparticles [13], for the two gradation profiles adopted in our manuscript  $|E|^2 = (gz + b)/\chi^{(3)}$ , the maximum pump fields intensities are  $I_m = |E|^2 = 61.5$  and  $72.1$  mW/cm<sup>2</sup> respectively. They are experimentally practical. The intensity of probe fields can be fraction of milliwatts per cm<sup>2</sup>, which is the requirement of the weak nonlinearity. When the probe fields are at 535 nm, and the thickness of each layer of the superlattice  $d_1 = d_2 = 75$  nm, the BO frequencies  $f_B = 1/T_B$  are 0.720 THz and 0.853 THz respectively. All the  $f_B$ 's are just located within the range of terahertz band, namely,  $10^{11} - 10^{13}$  Hz. For decoupling THz radiation from the structure, one can apply a uniform pump field to the structure, leading to the non-tilted band diagram. Meanwhile, the structure is illuminated by an incident light with frequency in the region of photonic allowed bands. Second, once the graded pump electric field is applied suddenly, the pulse propagating in the structure will be trapped and the oscillations commence subsequently. Third, after several oscillation periods, the graded pump field is restored to the uniform case, then the carrier waves with terahertz modulation can escape from the structure. Meanwhile, to avoid the leakage of energy in the transverse direction, spatial confinement is needed. In this regard, total internal reflection like in graded-index optical fibers can be used. For low-index medium, it is useful to guide light by means of a photonic band gap.

In summary, we have theoretically exploited the occurrence and tunability of PBOs in one-dimensional PCs containing nonlinear composites by applying graded external electric fields. Meanwhile, a kind of terahertz PBOs can appear and cover a terahertz band in electromagnetic spectrum.

*Acknowledgments.* This work was supported by the RGC Earmarked Grant of Hong Kong SAR Government, by the C. N. Yang Fellowship in CUHK, by the CNKBRSF under Grant No. 2006CB921706, by the Pujiang Talent Project (No. 06PJ14006) of the Shanghai Science and Technology Committee, by the Shanghai Education Committee ("Shu Guang" project), and by the NNSFC under Grant No. 10604014.

## References

1. F. Bloch, Z. Phys. **52**, 555 (1928); C. Zener, Proc. R. Soc. London A **145**, 523 (1934).
2. L. Esaki and R. Tsu, IBM J. Res. Dev. **14**, 61 (1970).
3. C. Waschke, H. G. Roskos, R. Schwedler, K. Leo, H. Kurz, and K. Köhler, Phys. Rev. Lett. **70**, 3319 (1993).
4. H. Sanchis-Alepuz, Y. A. Kosevich, and J. Sánchez-Dehesa, Phys. Rev. Lett. **98**, 134301 (2007).
5. L. Gutiérrez, A. Díaz-de-Anda, J. Flores, R. A. Méndez-Sánchez, G. Monsivais, and A. Morales, Phys. Rev. Lett. **97**, 114301 (2006).
6. R. Sapienza, P. Costantino, D. Wiersma, M. Ghulinyan, C. J. Oton, and L. Pavesi, Phys. Rev. Lett. **91**, 263902 (2003).
7. L. Smrčka, N. A. Goncharuk, M. Orlita, and R. Grill, Phys. Rev. B **76**, 075321 (2007).
8. V. Lousse and S. Fan, Phys. Rev. B **72**, 075119 (2005).
9. G. Wang, J. P. Huang, and K. W. Yu, Appl. Phys. Lett. **91**, 191117 (2007).
10. J. P. Huang and K. W. Yu, Phys. Rep. **431**, 87 (2006).
11. D. Ricard, P. Roussignol, and C. Flytzanis, Opt. Lett. **10**, 511 (1985).
12. G. Q. Gu and K. W. Yu, Phys. Rev. B **46**, 4502 (1992).
13. H. R. Ma, R. F. Xiao, and P. Sheng, J. Opt. Soc. Am. B **15**, 1022 (1998).
14. K. W. Yu, Solid State Commun. **105**, 689 (1998).
15. H. B. Liao, R. F. Xiao, J. S. Fu, P. Yu, G. K. L. Wong, and P. Sheng, Appl. Phys. Lett. **70**, 1 (1997).
16. P. St. J. Russell and T. A. Birks, J. Lightwave Technol. **17**, 1982 (1999).

## List of Figures

- 1 (Color online) Schematic view of the one-dimensional PC composed of a composite layer (nonlinear composites) with thickness  $d_1$  and a dielectric layer (e.g., air) with thickness  $d_2$ . The composites can be prepared with nonlinear nanoparticles (e.g., gold) randomly dispersed in a linear dielectric (e.g., silica), as shown in the right panel. For plotting Figs. 2-3, we shall use  $d_1 = d_2 = 0.5a$ , where  $a$  denotes the lattice constant. . . . . 7
- 2 (Color online) Depth-dependent photonic band structure for gradation profile  $\chi_p^{(3)} E_0^2 = gz + b$  with parameters  $g = 3.67 \times 10^{-4}$  and  $b = 1.33 \times 10^{-2}$  [which correspond to Fig. 3(a)]. The vertical dashed lines label the space of oscillations displayed in Fig. 3(a), for an incident wave with  $\omega_0 = 1.76 c/a$ . The cross section composed by the two horizontal dotted lines in the second band denotes the full region for the appearance of oscillations for various angular frequencies of incident electromagnetic waves. . . . . 8
- 3 (Color online) The time-dependent mean position and width of a wave packet under pump electric fields with different gradation profiles  $\chi_p^{(3)} E_0^2 = gx + b$ . The panels (a) and (c) correspond to  $g = 3.67 \times 10^{-4}$  and  $b = 1.33 \times 10^{-2}$ , (b) and (d) for  $g = 4.33 \times 10^{-4}$  and  $b = 1.33 \times 10^{-2}$ . The Bloch oscillations clearly develop around different centers with different periods. . . . . 9

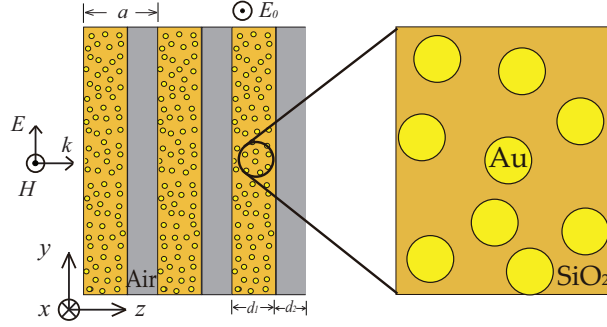


Fig. 1. (Color online) Schematic view of the one-dimensional PC composed of a composite layer (nonlinear composites) with thickness  $d_1$  and a dielectric layer (e.g., air) with thickness  $d_2$ . The composites can be prepared with nonlinear nanoparticles (e.g., gold) randomly dispersed in a linear dielectric (e.g., silica), as shown in the right panel. For plotting Figs. 2-3, we shall use  $d_1 = d_2 = 0.5a$ , where  $a$  denotes the lattice constant.

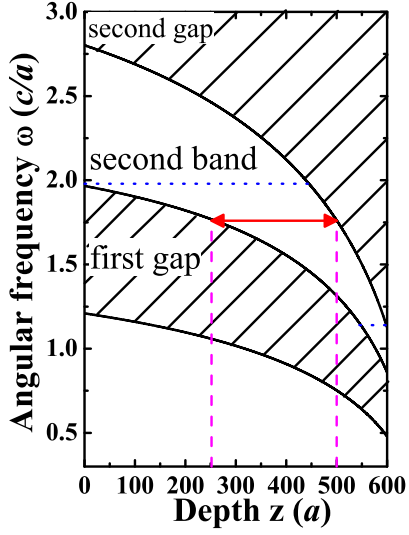


Fig. 2. (Color online) Depth-dependent photonic band structure for gradation profile  $\chi_p^{(3)} E_0^2 = gz + b$  with parameters  $g = 3.67 \times 10^{-4}$  and  $b = 1.33 \times 10^{-2}$  [which correspond to Fig. 3(a)]. The vertical dashed lines label the space of oscillations displayed in Fig. 3(a), for an incident wave with  $\omega_0 = 1.76 c/a$ . The cross section composed by the two horizontal dotted lines in the second band denotes the full region for the appearance of oscillations for various angular frequencies of incident electromagnetic waves.



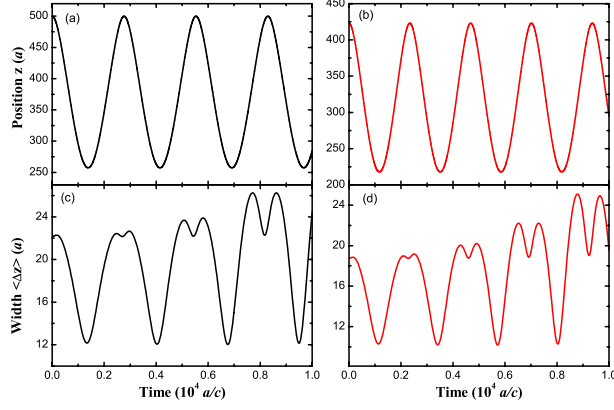


Fig. 3. (Color online) The time-dependent mean position and width of a wave packet under pump electric fields with different gradation profiles  $\chi_p^{(3)} E_0^2 = gx + b$ . The panels (a) and (c) correspond to  $g = 3.67 \times 10^{-4}$  and  $b = 1.33 \times 10^{-2}$ , (b) and (d) for  $g = 4.33 \times 10^{-4}$  and  $b = 1.33 \times 10^{-2}$ . The Bloch oscillations clearly develop around different centers with different periods.